Compact CPW-Fed Combline Filter in Substrate Integrated Waveguide Technology

Jorge D. Martínez, *Member, IEEE,* Stefano Sirci, Máriam Taroncher, and Vicente E. Boria, *Senior Member, IEEE*

***Abstract*—In this letter, the design and experimental results of compact low loss combline filters, based on the extension of the classical coaxial waveguide resonator to Substrate Integrated Waveguide (SIW) technology, are succesfully demonstrated. A $3-$pole 5% FBW Chebyshev filter has been designed, fabricated and measured. The fabricated device shows an excellent agreement with simulated results. These structures keep the low-cost fabrication scheme of single-layer PCB processing, while requiring less than half the area compared to a conventional SIW design.**

***Index Terms*—Microwave filter, compact filter design, combline resonator, substrate integrated waveguide.**

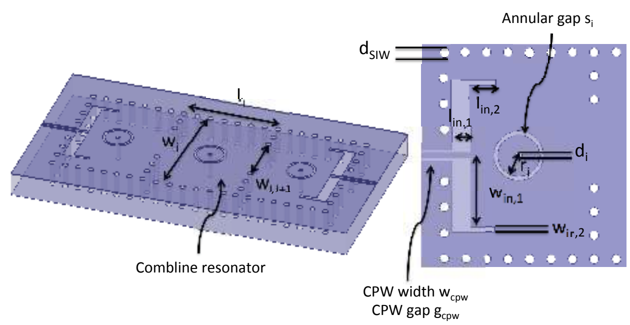

Fig. 1. Layout of the combline filter in SIW technology. Cavity and couplings dimensions are measured from via center to center.

I. Introduction

COMBLINE filters have been extensively used in metallic waveguide technology for implementing compact size filters. Although the insertion of metallic posts as perturbing elements of the TE_{101} mode in SIW circuits had been already explored in [1] for reconfiguration purposes, the authors have recently proposed that a combline resonator in SIW technology can be built by inserting an opened-shorted plated via hole inside the cavity [2].

In this letter, an X-band combline filter is succesfully designed, fabricated and measured in SIW technology. A model for the proposed resonator is considered, and a systematic procedure for the design of these miniaturized coupled resonator bandpass filters is presented. Measurements and simulation results are in good agreement, showing the potential advantages of this structure in terms of size, design flexibility and spurious rejection, without increasing insertion losses compared to its conventional SIW counterpart.

II. Analysis and design

A. TEM model and resonant frequency

The structure of the proposed combline SIW resonator is shown in Fig. 1. The inner via is short-circuited at the bottom metallization and open ended at the top. A capacitance is therefore established between a metallic disk, connected to the inner via, and the top metallization of the SIW cavity through the fringing fields accross an annular gap etched on the metal. Narrow bandpass filters can be implemented by inserting inductive windows coupling adjacent resonators.

The susceptance $B(\omega)$ of the resonator can be expressed as

$$B(\omega) = \omega C_d - Y_0 \cot \beta h \tag{1}$$

being C_d the capacitance between the disk and the top plane of the SIW cavity, Y_0 the characteristic admittance of the TEM mode short-circuited transmission line formed by the inner (circular) and outer (rectangular) conductors, $\beta = \frac{\omega\sqrt{\epsilon_r}}{c_0}$ the phase constant of the coaxial line at frequency ω, and h the substrate thickness.

The inductive contribution comes from the TEM mode short-circuited resonator, that can be seen as a short piece of coaxial transmission line of length h and characteristic admittance Y_0 embedded into the dielectric of permittivity ϵ_r. For a circular inner conductor of diameter d and a square contour of side w, the characteristic admittance can be well approximated when $w >> d$ by [3]

$$Y_0 = \left[\frac{60}{\sqrt{\epsilon_r}} \ln\left(1.079\frac{w}{d}\right)\right]^{-1} \tag{2}$$

Neglecting the thickness of the conductors, the capacitance established between the metal disk of radius r and the SIW top metal can be computed from [4]

$$C_d = \frac{2\pi r \epsilon_0 (1+\epsilon_r)}{\ln\left(1+\frac{s}{r}\right)} \int_0^{\infty} \left[J_0(\zeta r) - J_0(\zeta(r+s))\right] \frac{J_1(\zeta r)}{\zeta} d\zeta \tag{3}$$

where s is the annular gap and J_n the nth-order Bessel function of the first kind.

The resonant frequency can be obtained from the condition $B(\omega_0) = 0$. The field pattern of the first resonant modes of the

The authors would like to thank Generalitat Valenciana and MICINN (Spanish Government) for its financial support under projects GV/2009/007 and TEC2010-21520-C04-01.

J.D Martínez is with the I3M, Universitat Politècnica de València, Valencia, Spain. S. Sirci, M. Taroncher and V.E. Boria are with the Instituto de Telecomunicaciones y Aplicaciones Multimedia (iTEAM), Universitat Politècnica de València, Valencia, Spain.

Manuscript received x, xxxx.

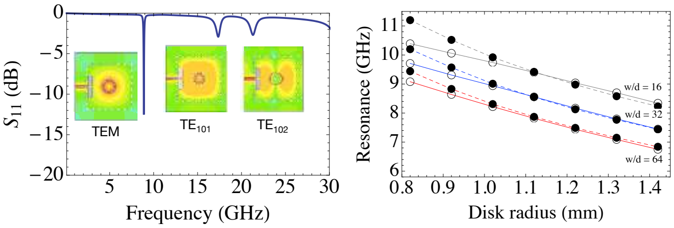

Fig. 2. First resonant modes of a combline cavity in SIW technology, and resonant frequency given by full-wave EM simulations (solid) and the TEM resonator model (dashed) as a function of the disk radius for different values of $\frac{w}{d}$ (right). Fixed resonator dimensions are $w = l = 8$ mm, $h = 1.524$ mm, $\epsilon_r = 3.55$, $s = 150$ μm. A better accuracy of the TEM model is obtained for higher values of r (and therefore of C_d), where the contribution of the via post is minimized.

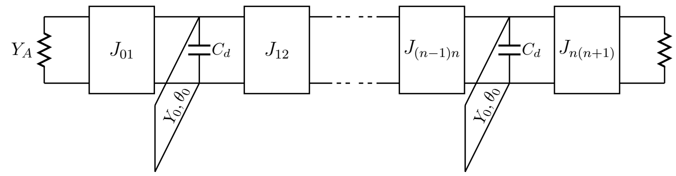

Fig. 3. Equivalent prototype of an N[th]-order combline resonator bandpass filter with frequency invariant admittance inverters.

combline resonator in SIW technology are shown in Fig. 2. As can be seen, the first spurious responses are those due to the perturbed TE$_{n0m}$ modes of the SIW cavity [5]. A comparison between the resonant frequency given by the TEM model of the resonator and the obtained using 3D full-wave simulations is also presented in Fig. 2, showing good agreement.

The input/output coupling to the resonator is realized through a modified coplanar waveguide (CPW) probe. The probe excites the TE$_{101}$ mode in the SIW cavity that couples to the TEM mode of the combline resonator. The probe is composed of a CPW to microstrip transition short-circuited to the SIW top plane. Two slots are added at the end of the microstrip to increase the coupling.

B. Filter design

The prototype of the combline bandpass filter using shunt resonators and frequency-invariant admittance inverters is shown in Fig. 3. Given a filter response with centre frequency $w_0 = \sqrt{\omega_H \omega_L}$ and bandwidth $\Delta\omega$, being ω_H and ω_L the upper and lower cutoff frequencies, the loading capacitance C_d and the admittance of the coaxial resonator Y_0 can be obtained by mapping the resonator susceptance and the admittance inverters of the bandpass filter with those of the low-pass prototype.

The former condition can be expressed as

$$B(\omega) = \omega' \left(\frac{b\frac{\Delta\omega}{\omega_0}}{\Omega_c} \right) \tag{4}$$

where b is the resonator slope parameter, ω' and $\Omega_c = 1$ rad/s the angular frequency and cut-off frequency of the low-pass prototype respectively. The level of b will impact the unloaded quality factor of the resonator, and must be a trade-off between low losses, compactness and feasibility of the synthesized values of C_d and Y_0.

Now, substituting (1) into (4) for the corresponding pass-band edge frequencies ($\omega' = \pm 1 \rightarrow \omega = \{\omega_H, \omega_L\}$), we can obtain

$$C_d = \left(b\frac{\Delta\omega}{\omega_0} \right) \frac{\cot\theta_H + \cot\theta_L}{\omega_H \cot\theta_L - \omega_L \cot\theta_H} \tag{5}$$

$$Y_0 = \left(b\frac{\Delta\omega}{\omega_0} \right) \frac{\omega_H + \omega_L}{\omega_H \cot\theta_L - \omega_L \cot\theta_H} \tag{6}$$

Finally, the admittance inverters can be computed from the low-pass prototype coefficients $g_0, g_1, ..., g_{n+1}$ using the well-known expressions [6]

$$J_{0,1} = \sqrt{\frac{Y_A \left(b\frac{\Delta\omega}{\omega_0} \right)}{g_0 g_1}} \qquad J_{n,n+1} = \sqrt{\frac{Y_A \left(b\frac{\Delta\omega}{\omega_0} \right)}{g_n g_{n+1}}} \tag{7}$$

$$J_{i,i+1} = \left(b\frac{\Delta\omega}{\omega_0} \right) \sqrt{\frac{1}{g_i g_{i+1}}} \tag{8}$$

for $i = 1$ to $(n-1)$, where Y_A is the admittance of the input/output access ports.

Following this approach, a 3−pole Chebyshev filter centered at 9.8 GHz with 5% FWB and 0.05 dB in-band ripple has been synthesized. A substrate thickness $h = 1.524$ mm and permittivity $\epsilon_r = 3.55$ have been considered. Thus, a loading capacitance $C_d = 0.2$ pF and resonator admittance $Y_0 = 8.22$ mS have been obtained for a susceptance slope parameter $b = 0.014$ S. The inverter values are $J_{01} = J_{34} = 0.0036$ and $J_{12} = J_{23} = 0.0007$ for an input/output impedance $Z_A = 65$ Ω. The synthesized response can be seen in Fig. 5.

C. Layout

Firstly, the resonators are dimensioned. The diameter of the inner via d is chosen sufficiently small in order to reduce the size of the cavity for a given admittance level. However, this will be ultimately limited by the minimum via size of the fabrication process and its tolerances. The dimensions of a square SIW cavity with the synthesized admittance Y_0 can be obtained from (2). Next, given the required loading capacitance, the disk radius and annular gap can be obtained numerically from (3). Again, the minimum annular gap will be also limited by the fabrication process and the tolerances.

Once the resonators are designed, the input/output and inter-resonators couplings are dimensioned. The Q_{ext} and $k_{i,j}$ coefficients are obtained from the synthesized $J_{i,i+1}$ as

$$Q_{e,1} = \frac{bY_A}{J_{0,1}^2}, \qquad Q_{e,n} = \frac{bY_A}{J_{n,n+1}^2}, \qquad k_{i,i+1} = \frac{J_{i,i+1}}{b} \tag{9}$$

for $i = 1$ to $(n-1)$.

Then, using full-wave EM simulations, the external quality factor can be estimated from the group delay of the reflected response of a singly-loaded cavity [7]. For a given CPW-to-microstrip transition, the length of the slots $l_{in,2}$ is modified in order to increase the coupling. The coupling coefficient can also be obtained from the reflected response of two coupled

TABLE I
LAYOUT DIMENSIONS OF THE DESIGNED FILTER

l_1, l_3	5.85 mm	d_1, d_2, d_3	250 μm
l_2	6.02 mm	w_{12}, w_{23}	4.34 mm
w_1, w_2, w_3	8 mm	$l_{in,1}$	0.7 mm
r_1, r_3	0.8 mm	$l_{in,2}$	1.01 mm
r_2	0.85 mm	$w_{in,1}$	2.65 mm
s_1, s_2, s_3	150 μm	$w_{in,2}$	0.2 mm
w_{cpw}	200 μm	g_{cpw}	100 μm
d_{SIW}	350 μm		

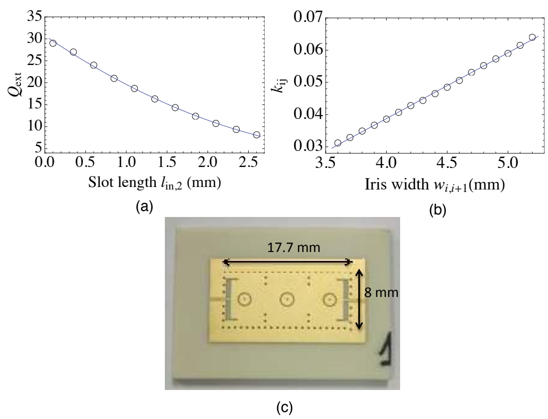

Fig. 4. (a) Q_{ext} as a function of the input/output slot length, (b) k_{ij} versus iris width, and (c) photography of the fabricated filter.

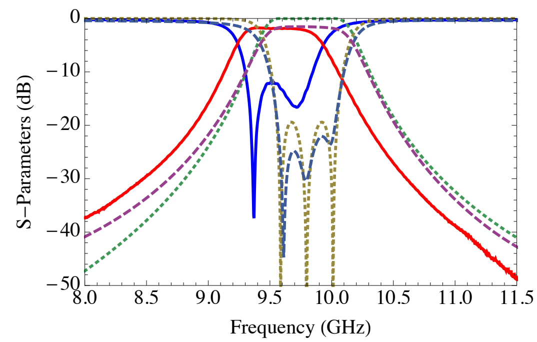

Fig. 5. Measured (solid), simulation (dashed) and synthesized (dotted) response of the 5% FBW 3−pole Chebyshev filter.

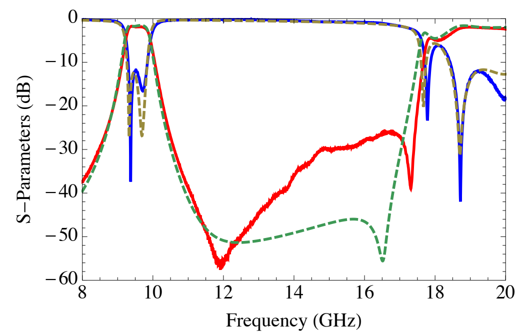

Fig. 6. Measured (solid) and simulated (dashed) wideband response of the fabricated filter considering the finite metallization thickness.

singly-loaded cavities. The coupling between both resonators is obtained as a function of the iris width. The Q_e and $k_{i,j}$ curves for the designed filter can be seen in Fig. 4.

Finally, a fine-tuning procedure is performed using full-wave EM simulations. During this process, the characteristic admittance and loading capacitance of the resonators must be slightly modified due to the loading effect of the inverters. Both distributed circuit parameters are finely controlled through the modification of the disk radius and the SIW cavity lengths. The layout dimensions of the previously synthesized filter are shown in Table I. The EM simulated response of the filter compared to the synthesized model can be seen in Fig. 5.

III. EXPERIMENTAL RESULTS

The filter was fabricated in a 1.524 mm thick Rogers RO4003C substrate ($\epsilon_r = 3.55$, $\tan\delta = 2.7 \cdot 10^{-3}$) using standard single-layer PCB processing technology. Filter size is 17.7×8 mm^2, while the equivalent conventional SIW filter would require about 36×12 mm^2 for square cavities using the dominant TE_{101} mode. The device was measured using a network analyzer on a probe station with GSG 250 μm pitch probes, and S-parameters were re-normalized to the port impedance of 65Ω. Results can be seen in Fig. 5, showing mid-band insertion losses of 1.7 dB with measured 1-dB bandwidth of 5.8%.

The filter pass-band has been shifted to lower frequencies due to an increased capacitive effect, that is coming from the thickness of the SIW metallization associated to the parallel-plate capacitance and the fringing fields at the edges of the metal layer. The thickness of the metallization has been measured and incorporated into the EM simulations, showing excellent agreement with the measurements as can be seen in Fig. 6. Wideband response of the filter shows a spurious-free band of almost one octave with a rejection level better than 30 dB up to 17 GHz.

IV. CONCLUSIONS

The design, performance and manufacturability of novel combline filters in SIW technology have been demonstrated. The measured results show excellent agreement with the EM simulations when all involved physical effects are considered. The proposed topology presents imporant advantages in terms of size compactness, spurious rejection and design flexibility.

REFERENCES

[1] J.C. Bohorquez, B. Potelon, C. Person, E. Rius, C. Quendo, G. Tanne and E. Fourn, "Reconfigurable planar SIW cavity resonator and filter", *IEEE MTT-S International Microwave Symposium Digest*, Jun. 2006, pp. 947 − 950.

[2] J.D. Martínez, M. Taroncher and V.E. Boria, "Capacitively loaded resonator for compact substrate integrated waveguide filters", in *Proc. 40th Eur. Microw. Conf.*, Sep. 2010, pp. 192 − 195.

[3] H.J. Riblet, "An accurate approximation of the impedance of a circular cylinder concentric with an external square tube", *IEEE Trans. Microw. Theory Tech.*, vol. 31, no. 10, pp. 841 − 844, Oct. 1983.

[4] H.S. Lee and H.J. Eom, "Potential distribution through an annular aperture with a floating inner conductor", *IEEE Trans. Microw. Theory Tech.*, vol. 47, no. 3, pp. 372 − 374, Mar. 1999.

[5] D. Deslandes and K. Wu, "Accurate modeling, wave mechanism, and design consideration of a substrate integrated waveguide", *IEEE Trans. Microw. Theory Tech.*, vol. 45, no. 6, pp. 2516 − 2526, Jun. 2006.

[6] J. S. Hong and M. J. Lancaster, *Microstrip filters for RF/Microwave Applications*, New York: Wiley, 2001.

[7] J.B. Ness, "A unified approach to the design, measurement and tuning of coupled-resonator filters", *IEEE Trans. Microw. Theory Tech.*, vol. 46, no. 4, pp. 343 − 351, Apr. 1998.